Journal of Metals, Materials and Minerals, Vol. 31, No. 3, pp. 53-62, 2021

The effect of artificial defects on the fatigue characteristics of AISI 4340 steel

Yaakov B. UNIGOVSKI[1,*], Dmitry FISHMAN[2], Liat FISHMAN[1], Liron SHICHMAN[1], Ofir MOSHE[1], Roni Z. SHNECK[1], and Emmanuel M. GUTMAN[1]

[1] *Ben-Gurion University of the Negev, 84105, Department of Materials Engineering, Beer-Sheva, Israel.*
[2] *Materials Science and Engineering Division, Depot 22, Israel Air Force, P.O. Box 02538, Tel Aviv, Israel.*

***Corresponding author e-mail:** yakovun@bgu.ac.il

Received date:
24 April 2021
Revised date
18 August 2021
Accepted date:
20 August 2021

Keywords:
Low alloy steel;
High cyclic fatigue;
Surface roughness;
Artificial defects;
Shot peening

Abstract

This study examined the fatigue life (N_f) and fatigue limit (FL) of AISI 4340 steel in relation to surface roughness, artificial defects and shot peening. Artificial surface defects on fatigue specimens were obtained by electrical discharge machining (EDM) or by pre-corrosion in 3.5% NaCl and perchloric acid solutions, followed by a fatigue test. The presence of artificial defects of various sizes, taken into account by the $\sqrt{area}$ parameter, led to a significant decrease in fatigue characteristics, while shot peening contributed to their noticeable improvement. Defects resulting from electrochemical corrosion had a much greater negative effect on fatigue life than defects introduced by EDM.

1. Introduction

The fatigue (endurance) limit, also known as fatigue (endurance) strength, is associated with the phenomenon that crack nucleation is arrested by the first grain boundary or the dominant microstructural barrier [1]. The fatigue life as a number of cycles to failure (N_f) refers to the life required to nucleate and grow a small crack to the visible length of the crack and catastrophic destruction. When structural components are subjected to cyclic loads, the greatest stress occurs on the surface, especially in the presence of stress concentrators, where fatigue cracks occur and grow until the component breaks. As stress concentrators, they may be surface flaws that occur during the manufacturing (casting, machining, etc.); nonmetallic inclusions, secondary phases, cracks, as well as corrosion pits.

Since the effect of defects on the fatigue limit is so complex, no unifying method has been proposed for quantifying them. Therefore, a quantitative assessment of the influence on fatigue resistance of a defect can be established only by evaluating such an effect of an equivalent crack [1,2]. The characteristics of the dependency of stress intensity factors on the shapes of various three-dimensional cracks were proposed by Murakami, and a geometrical parameter was introduced that will control the fatigue limit [3]. This parameter, as a representative dimension (length), is the square root of the area ($\sqrt{area}$) of the defect projected in the direction of the maximum tensile stress. It is found that the maximum stress intensity factor along a three-dimensional crack is approximately proportional to $(\sqrt{area})^{1/2}$. To demonstrate the usefulness of the proposed parameter ($\sqrt{area}$), Murakami and Endo performed fatigue tests of samples containing very small holes, with diameters of 40 μm to 500 μm, and obtained quantitative relationships in the form: $\sigma_w^n\sqrt{area} = C$ for several materials, where σ_w is the fatigue strength (indicated below as the fatigue limit FL) and n = 6 [3,4].

Metal defects can be formed both during the machining of parts and during operation, when the properties of the metal degrade up to the destruction of products due to static (creep) or dynamic fatigue, as well as the influence of aggressive media. For example, fatigue limits are reduced by pitting corrosion up to half or less levels of non-corrosive strength levels [2]. As reported by Cammett and Prevey, corrosion of as-machined samples of 4340 steel in salt fog for 100 h and 500 h reduces the fatigue limit by 26% and 50%. Sometimes, quite superficial pitting as small as 0.025 mm has caused initiation of fatigue cracking in aluminum and steel aircraft components [5].

Several types of surface artificial flaws were used to evaluate the behavior of a fatigue crack, e.g., flaws obtained by drilling, indentation, electro-erosion (EDM), or using a focused ion beam (FIB) as well as corrosion pits introduced by the preliminary corrosion procedure [3-11]. First, to assess the non-propagating limit of small fatigue cracks, defects with a low stress concentration, such as drilled-holes, might not be able to be used, since no non-propagating crack arises from the flaw at the fatigue limit [6]. In addition, the creation of surface flaws can affect the material properties. In particular, a surface defect obtained by indentation appears to induce a relatively large change of the residual stress field [10]. The effect of various types of small artificial defects (circumferential notches, corrosion pits, drilled holes and pre-cracked holes) on the fatigue strength of 17 to 4 PH stainless steel was studied by Schönbauer *et al.* [7]. It was shown when FL of specimens with artificial defects is determined by the threshold

condition for the propagation of a crack, the shape and dimension of the defects can be evaluated using a $\sqrt{area}$ parameter. However, this method for evaluating non-detrimental defects is not necessarily applicable to the blunt or round defects, for which the fatigue limit is determined by the intensity range of the threshold stress of a long crack, ΔK_{th}. For example, a sample with a 0.1-mm-drilled-hole ($\sqrt{area}$ = 69 μm) failed after 1.2×10^8 cycles due to a crack emanated from a much smaller non-metallic inclusion with $\sqrt{area}$ = 13 μm [7].

Shot peening (SP) is a widely used surface treatment of alloys for improving fatigue strength of components [12,13]. It consists in impacting the surface by a flow of shots with kinetic energy sufficient to induce plastic deformation and to introduce compressive residual stresses and hardening of the material on the surface of the component and directly below it. These effects are useful for stopping or preventing crack propagation. SP can change mechanical properties of a metal, namely the surface profile, distribution of hardness and residual stress, grain refinement, etc. [8-10,13-15]. For example, for annealed medium-carbon steel without and with a wedge-shaped notch (radius of curvature 3 mm, $\sqrt{area}$ 50 mm), fatigue limit increased after SP by 27% and decreased by 9% for untreated samples, respectively. Thus, for samples with a small wedge-shaped defect subjected to shot peening, a total improvement in fatigue limit of 36% was obtained [8]. As reported in [9], a crack-like surface defect (a semicircular slit) up to 0.2 mm deep in high-strength steel can be neutralized with SP (300% coverage, 0.5 mA arc height). The fatigue limit of shot peened specimens with a slit is almost the same as for non-slit SP specimens. Meanwhile, untreated samples (un-SP) with such a defect have a fatigue limit of 56% less than for samples subjected to SP [9].

An analysis of the literature showed that the effect of artificial defects caused by corrosion on the fatigue properties of shot peened steels is not well understood. This research is aimed to studying the effect of corrosive shallow pits, surface roughness and shot peening on the fatigue behavior of low-carbon high-strength 4340 steel.

2. Experimental and methods

Hourglass–shaped samples (Figure 1) made of low-alloyed AISI 4340 steel (0.40% C, 0.25% Si, 0.70% Mn, 1.80 Ni, 0.80% Cr, 0.25% Mo, 0.025% S, and 0.025% P) were obtained on a CNC lathe, and then grinded with silicon carbide paper (grades 320, 500 and 800). After that, the samples were subjected to heat treatment in accordance to the standard SAE AMS-H-6875B (quenching in vacuum at 840°C for 85 min with cooling in argon, and tempering at 490°C for 150 min

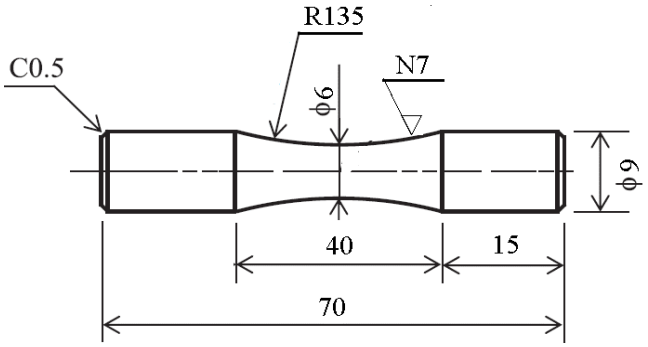

Figure 1. The dimensions of the fatigue specimen, mm.

in air). Ultimate tensile strength (UTS), tensile yield strength (TYS) and elongation-to-fracture were 1270 MPa, 1040 MPa and 11%, respectively. The hardness of the samples after heat treatment was 40.0 HRC to 42.5 HRC (≈HV405). After heat treatment, the samples were ground using SiC 1000 grad paper with roughness parameters R_a equal to 0.4 μm. The surface of some samples with R_a values of about 1.6 μm was not treated with SiC paper to compare the effects of roughness and pre-corrosion on the life of the steel when tested for HCF.

The shot peening was performed using S230 cast steel shot media with a diameter of 0.6 mm in on a Pangborn shot peening machine with a peening intensity of 0.008 A to 0.012 A (≈0.24 mmA). The diameter of the peening nozzle was 9.5 mm (3/8"), and the distance between the nozzle and sample was 275 ± 25 mm. The incident angle was 40° to 50°, and the SP coverage was 100%.

Artificial defects (pits) were obtained using anodic dissolution of steel in an electrochemical cell and using an electric-discharge machine (EDM). In addition, one sample, in the central portion of which there are three prints obtained with a Rockwell 120-degree diamond indenter during hardness tests, was tested in a bending fatigue experiment. The electrochemical cell for preliminary pitting corrosion of fatigue samples consisted of two electrodes, where the sample and the graphite rod were used as the anode and cathode, respectively. The following two solutions were used as electrolytes: 0.6 M NaCl and a solution for electrolytic polishing, based on perchloric acid $HClO_4$, including per liter: 60 mL -70% $HClO_4$; 800 mL -95% ethanol and 140 mL distilled water [16]. The parameters for creating artificial pits were as follows: constant voltage 12 V to 20 V; current 0.5 A to 6.0 A; the duration is 0.8 min to 6.0 min with a distance of about 2 mm between the graphite cathode and the surface of the fatigue sample.

Table 1. Surface characteristics of samples of tempered 4340 steel.

Group	Roughness, R_a (μm)	State of the surface	$\sqrt{area}$ min/max (μm)
1	1.6	Without artificial defects	-
1a	1.6	Pits obtained using a perchloric acid solution (PA)	40/105
2	0.4	Without artificial defects	-
2a	0.4	With pits obtained in a NaCl solution	130/220
2b	0.4	With prints obtained in a hardness tests	270/275
3	0.4*	Shot peening (SP),without artificial defects	65/70**
3a	0.4*	SP, with pits obtained in a PA solution	18/230
3b	0.4*	SP, with pits obtained using EDM	52/140

Notes : * roughness before shot peening, ** no defects; $\sqrt{area}$ values show sizes of SP craters.

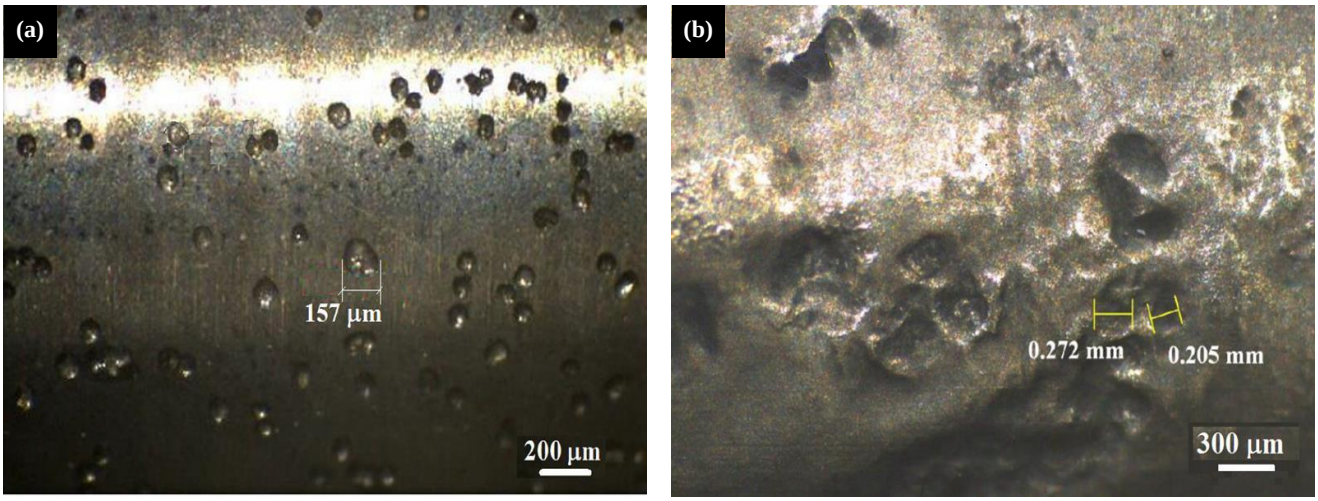

Figure 2. Artificial shallow pits produced by an anodic dissolution of samples in solutions of perchloric acid (a) and 3.5% NaCl (b)..

Additionally, small pits of controlled size in the center of the samples were obtained using EDM with a nominal depth varying from of 20 μm to 82 μm and a diameter of 137 μm to 240 μm (values $\sqrt{area}$ are 52, 95 and 140 μm). The surface parameters of samples before fatigue tests are shown in Table 1. In addition, in Figure 2, optical micrographs show small pits obtained in two electrolytes.

Fatigue tests were performed at 25°C ± 1°C and a frequency of about 50 Hz using a rotating beam type (R = -1) fatigue machine (Satec System, Inc., USA) with uniform bending moment. Fatigue limit (strength) was defined as the maximum nominal rotary bending stress, at which the specimen withstood 10^7 or more cycles. Microstructure studies were carried out using a NICON optical microscope and a JEOL JSM-5600 scanning electron microscope with a NORON energy dispersive spectroscope.

3. Results and discussion

3.1 Effect of load and surface defects on the fatigue life and fatigue limit of steel

The S-N diagram (Figure 3) and Table 2 show the results of high-cycle fatigue tests, carried out using samples with different surface characteristics. Due to the usual spread of data for the fatigue life N_f, the results obtained for fractured samples of all three groups were approximated by Equations (1)-(3), respectively. As expected, the roughness of the fatigue samples is a critical factor for the fatigue performance of steel. For example, samples of group 1 with a roughness of 1.6 μm have an order of magnitude lower fatigue life compared to samples of group 2 with R_a of 0.4 μm: 10^5 and 10^6 cycles, respectively, at the same applied stress of 624.8 MPa (Figure 3).

$$logN_1 = 6.685 - 2{,}795 \times 10^{-3}\,\sigma, \quad R^2 = 0.998 \qquad (1)$$

$$logN_2 = 12.236 - 9.727 \times 10^{-3}\,\sigma, \quad R^2 = 0.811 \qquad (2)$$

$$logN_3 = 13.984 - 1.146 \times 10^{-2}\,\sigma, \quad R^2 = 0.785 \qquad (3)$$

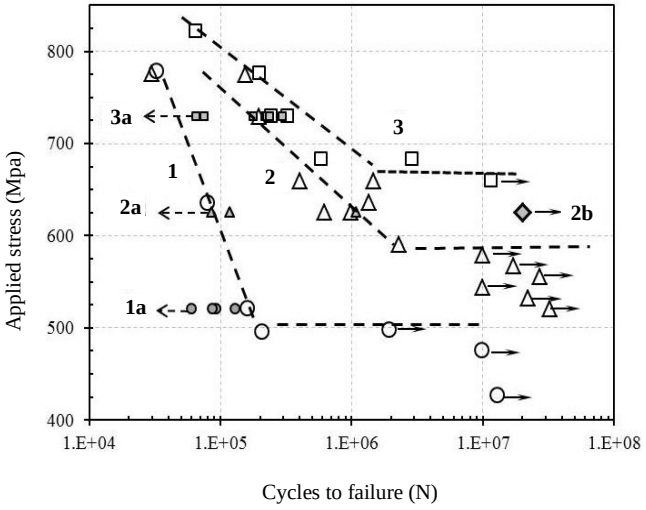

Figure 3. S-N diagram for untreated (1, 2) and shot peened (3) AISI 4340 steel specimens, with the surface roughness R_a 1.6 (1) and 0.4 (2,3) μm. The designations filled in gray refer to specimens with artificial defects of groups: 1a (circles), 2a (triangles), 2b (a rhombus), and 3a (squares).

Shot peening lead to an additional increase in the fatigue characteristics of 4340 steel. An estimation of the effect of surface parameters on the fatigue life, which has a common data spread, can be performed for all three groups of samples using Equation (1)-(3). For instance, at an applied stress of 700 MPa, the average fatigue life N_f is (0.54; 2.7 and 9,1) $\times 10^5$ cycles to failure for groups of 1, 2 and 3, respectively. Thus, in other words, with such a high stress, the improvement in surface finish between group 1 and group 2, where R_a is 1.6 and 0.4 μm, respectively, led to an increase in N_f by 5 times.

Additionally, the hardening of the surface of samples of group 3 by the method of shot peening as compared with group 2, led to an increase in N_f by a factor of 3.4. Similar results were reported by Wu *et al.*, where for smooth and SP samples of the GH4169 superalloy, the average N_f values increased from 0.6×10^5 to 3.0×10^5 cycles at the stress of 900 MPa [15].

Table 2. Surface characteristics of fatigue samples without and with artificial defects, and the results of fatigue tests.

Group	Sample No.	Pit dia. (μm)	Pit depth (μm)	$\sqrt{area}$ (μm)	Stress (MPa)	$N \times 10^{-5}$ (cycles)	Notes
1	L3	-	-	-	335.6	113.00	runout
	Z11	-	-	-	425.8	130,00	runout
	Z15	-	-	-	474.4	100,00	runout
	Z13	-	-	-	495.2	2,10	runout
	Z17	-	-	-	497.6	19,70	runout
	L10	-	-	-	520.7	70,00	runout
	L4	-	-	-	520.7	2,40	fracture
	L11	-	-	-	520.7	1,90	fracture
	Z14	-	-	-	520.7	1,62	fracture
	Z16	-	-	-	635.3	0.80	fracture
	Z12	-	-	-	777.6	0.33	fracture
	L1	-	-	-	798.4	0.20	fracture
1a*	L8	221	-	-	520.7	0.93	fracture
	L5	172	-	-	520.7	0.87	fracture
	L7	157	-	-	520.7	0.60	fracture
	L9	77	-	-	520.7	1.30	fracture
2	1	-	-	-	520.7	324.0	runout
	2	-	-	-	532.3	220.0	runout
	3	-	-	-	543.8	100.0	runout
	4	-	-	-	555.4	270.0	runout
	5	-	-	-	567.0	170.0	runout
	6	-	-	-	590.1	23.2	fracture
	7	-	-	-	624.8	9.91	fracture
	8	-	-	-	624.8	6.16	fracture
	9	-	-	-	636.4	13.60	fracture
	10	-	-	-	659.6	4.05	fracture
	11	-	-	-	659.6	14.60	fracture
	12	-	-	-	729.0	1.98	fracture
	13	-	-	-	775.3	1.55	fracture
	14	-	-	-	775.3	0.30	fracture
2a	15	148/595**	30	130	624.8	10.08	fracture
	16	352	154	220	624.8	0.86	fracture
	17	195	172	180	624.8	1.19	fracture
2b	18	585	129	275	624.8	200.00	runout
3	20	-	-	70	659.6	116.60	runout
	23	-	-	70	682.7	29.19	fracture
	25	-	-	70	682.7	5.96	fracture
	19	-	-	70	729.0	2.47	fracture
	24	-	-	70	729.0	3.07	fracture
	21	-	-	70	775.3	2.00	fracture
	26	-	-	67	821.5	0.66	fracture
3a	22	120	77	96	729.0	3.00	fracture
	27	18	20	19	729.0	2.25	fracture
	28	195	11	46	729.0	2.20	fracture
	29	58	25	40	729.0	1.78	fracture
	30	460	122	230	729.0	0.65	fracture
	31	32	10	18	729.0	2.28	fracture
	32	95	95	95	729.0	0.75	fracture
	33	15	92	11	729.0	2.39	fracture
3b	34	137	20	52	729.0	5.17	fracture
	35	170	54	95	729.0	3.65	fracture
	36	240	82	140	729.0	2.16	fracture

Notes: * In group 1a, the depth of the pits was not measured. ** The pit was elliptical.

As shown in Figure 3, the fatigue limit of tempered steel 4340 with different surface properties (Table 1) is 500, 580 and 660 MPa for samples of groups 1, 2 and 3. Thus, an improvement in surface finish with a decrease in the roughness R_a of samples from 1.6 μm to 0.4 μm led to an increase in fatigue limit by 16%. In addition, due to shot peening, FL increases from 580 MPa to 660 MPa (+13.8%) for samples with the same initial roughness of 0.4 μm (Figure 3). The same trend was reported for steel with a chemical composition similar to steel 4340, for which the SP method led to an increase in FL by 9% [9].

As is known from the literature, the fatigue limit strongly depends on the surface roughness [1,2,17-19]. According to [1], the FL estimate shows that for steel with UTS 1270 MPa, as in our case, the surface finish factor C_s is 0.89; 0.78 and 0.67 for a surface roughness of 0.4; 1.6 μm and 3.2 μm. For example, for very-high strength steel (Ni–Cr–Mo) with a decrease in R_a from about 2.6 μm to 1.4 μm, the FL value increased from 850 MPa to 1000 MPa (+17.6%) [17]; the same tendency was found for both the 7010 aluminum alloy [18] and the Ti-Al-4V alloy [19].

The empirical relationship between the fatigue limit and Vickers hardness (HV) is known (Equation (4)) for steels with HV < 400, where HV is the Vickers hardness number [20,21]. Considering the $\sqrt{area}$ parameter for samples with defects, this equation was transformed by Murakami in his model into an Equation (5) [4,21], where HV is the Vickers number and the $\sqrt{area}$ parameter in μm. We should only be noted the inaccuracy in the description of Equations (4) and (5) in [4,7,17,19,21], in which the hardness HV is indicated in kgf·mm^{-2} instead of the dimensionless HV, as shown in Figure 4 [20].

$$FL, _{ideal} = 1.6\,HV \pm 0.1\,HV, MPa \quad (4)$$

$$FL = 1.43\,(HV + 120)\,(\sqrt{area})^{-1/6}, MPa \quad (5)$$

The ideal fatigue limit calculated by Equation (4) is 648 ± 40 MPa at HV405. Given a surface finish factor of 0.89 [1] for group 2 (R_a = 0.4 μm, UTS = 1270 MPa), we have FL, $_{ideal}$ = FL/C_s = 580/0.89 = 652 MPa, which is consistent with the values obtained from Equation (4). The same estimate for group 1 (R_a = 1.6 μm, C_s = 0.78) gives an ideal FL value of 641 MPa, which is also consistent with Equation (4). As follows from Figure 5, the presence of artificial defects of various sizes, which are taken into account by the $\sqrt{area}$ parameter, led to a significant decrease in the fatigue life of the samples and the fatigue limit calculated by Equation (5).

For example, at the same stress of 729 MPa, the average N_f value for control samples of group 3 calculated by Equation (3), is 4.4×10^5 cycles. However, in the presence of pits obtained as a result of preliminary corrosion in a solution of perchloric acid (group 3a), N_f ranged from 0.65×10^5 cycles to 3.0×10^5 cycles or reduced by about 1.5 times to 7 times depending on the $\sqrt{area}$ parameter, which varied from 11 μm to 230 μm, respectively (Table 2). According to Equation (5), the fatigue limits for samples with $\sqrt{area}$ parameters of 5, 50 and 500 μm is 574, 391 and 266 MPa, respectively.

Shot peening of samples with defects (groups 3a, 3b) significantly reduces the dependence of fatigue life on the $\sqrt{area}$ parameter compared to untreated samples of group 2a. Defects obtained by electrochemical corrosion had a much greater detrimental effect on fatigue life compared with defects obtained using the EDM technique (Figure 5, curves 3 and 2). For example, as follows from Figure 5 and Table 2, a fivefold decrease in fatigue life (3.65×10^5 cycles and 0.75×10^5 cycles) was revealed in the presence a defect resulting from electrochemical corrosion compared with a defect obtained by EDM, under the same conditions (σ = 729 MPa, $\sqrt{area}$ = 0.095 mm).

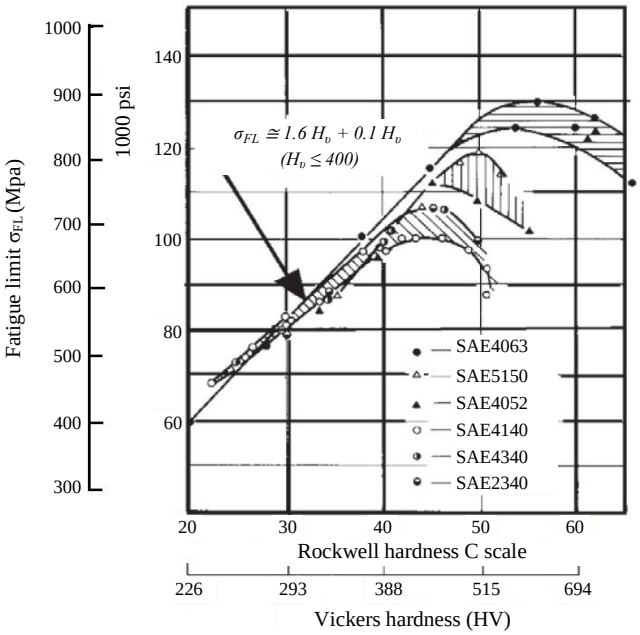

Figure 4. Relationship between hardness and the fatigue limit (zero mean stress) [20].

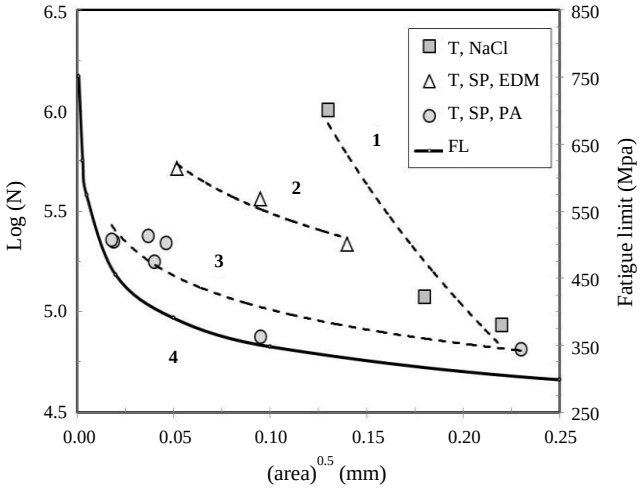

Figure 5. The effect of the $(area)^{0.5}$ parameter on the fatigue life (1-3) and fatigue limit (4), calculated by Eq (5) for tempered (T) and shot peened (T, SP) specimens with artificial defects obtained using electrochemical corrosion in NaCl and perchloric acid solutions, as well as EDM.
Groups (Tables 1, 2): 2a (1); 3b (2); 3a (3). σ, MPa: 624.8 (1) and 729.0 (2, 3)

3.2. Characterization of fatigue fracture surface of samples with defects

A fractographic examination is of interest for a qualitative analysis of the effect of various surface defects as the origins of the failure and micro- and macrostructural constituents on fatigue life. As is known and shown in Figure 6, the fracture surface of samples consist usually of three main zones: crack initiation zone (I), crack propagation zone (II) and zone of sudden (final) fracture (III). In the presence of the

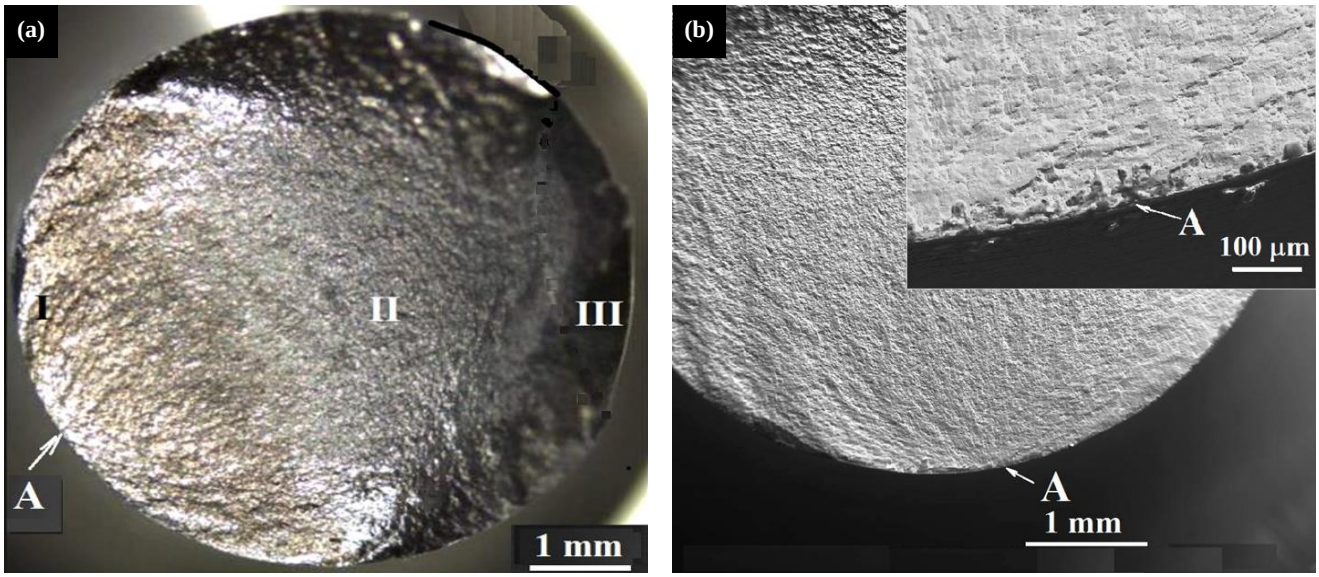

Figure 6. The fracture surface of the sample, showing the zones of initiation of cracks (I), propagation of cracks (II) and final (III) fracture (a), and as well as a magnification of the area I near the origin of crack A (b) (sample L10, group 1, 520.7 MPa, 7×10^6 cycles).

surface heterogeneities, the initiation and growth of fatigue crack during Stage I occurs mainly as a result of the slip-plane cracking at these sites, and up to 90% of the fatigue life may be spent to initiate a viable fatigue crack [22]. Stage III is the final propagation phase of a fatigue crack, which, as a rule, is characterized, as a rule, by ductile rupture due to microvoid coalescence. During this stage, the crack growth rate increases until the fatigue crack becomes unstable, and the part fails by overload mechanism.

Typically, the area of zone III increases with increasing applied stress, since the relative high overload leads to an increase in the crack propagation rate and the sudden failure of the samples. For samples without and with shot peening, including samples with previously prepared pits (groups 2, 2a and 3), it was found that, despite a certain scatter of the results, the fraction of the area III of the final ductile fracture (A_d/A) of samples with different surface characteristics increases from 0.04 to about 0.20 with increasing load from 590 MPa to 821 MPa (Figure 7).

Let us consider the features of the initial fracture of samples with surface defects, to which we conditionally refer also craters (dents) caused by shot peening. Here, undoubtedly, the positive effect of hardening of the surface layer by shot blasting prevails over the detrimental effect of increasing surface roughness by dents, with the exception of fatigue failure at very high applied stresses. For example, in sample No. 26 at a maximum stress level of 821.5 MPa, as clearly shown in Figure 8(a) and 8(b), crack initiation occurred from several points. The start of the crack propagation point was point A, then there were other sources nearby, which are indicated by letter B and craters C1, C2. In general, Figure 8 illustrates the zones of an initial crack formation at stage I from artificial surface irregularities such as shot peening dents (a, b); a pit made by the EDM method (c, d), and, finally, from prints made during hardness tests (e, f).

Compared to samples without surface defects, samples with defects obtained by the electro-erosive method show only a slight decrease in fatigue life. For example, with the same applied stress of 729 MPa, the average N_f values for samples 19 and 24 from group 3 were 2.8×10^5 cycles or 4.3×10^5 cycles in accordance with Equation 3; meanwhile, sample No.36 with a hemispherical defect, made by the electroerosive method with an $\sqrt{\text{area}}$ parameter of 140 μm, showed a fatigue life of 2.2×10^5 cycles (Table 2, Figure 8(c), (d)). However, samples 27, 28 and 31 with defects resulting from pre-corrosion in a perchloric acid showed the same N_f level (about 2.3×10^5 cycles) at a much lower $\sqrt{\text{area}}$ parameter, which ranged from 18 μm to 45 μm (Table 2). Thus, as mentioned above, the defect obtained using preliminary electrochemical dissolution is much more harmful than the defect created by the EDM (Table 2, Figure 5, curves 3 and 2).

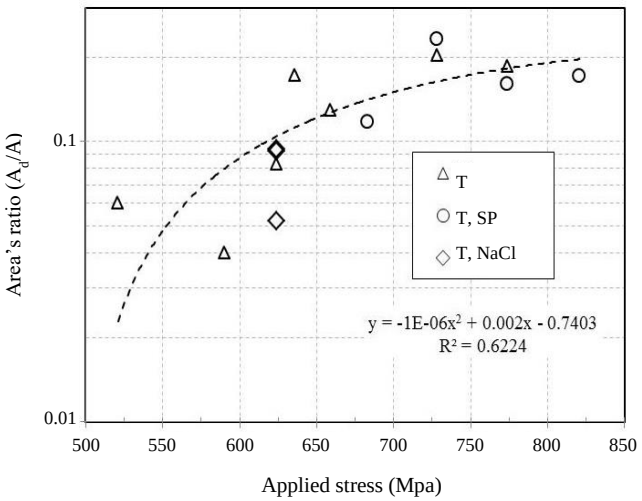

Figure 7. Effect of applied stress on the relative area of final (ductile) fatigue failure of samples of groups 2, 2a and 3 subjected to preliminary tempering (T), tempering and pre-corrosion in 0.6 M NaCl (T, NaCl) and tempering and shot peening (T, SP), respectively.

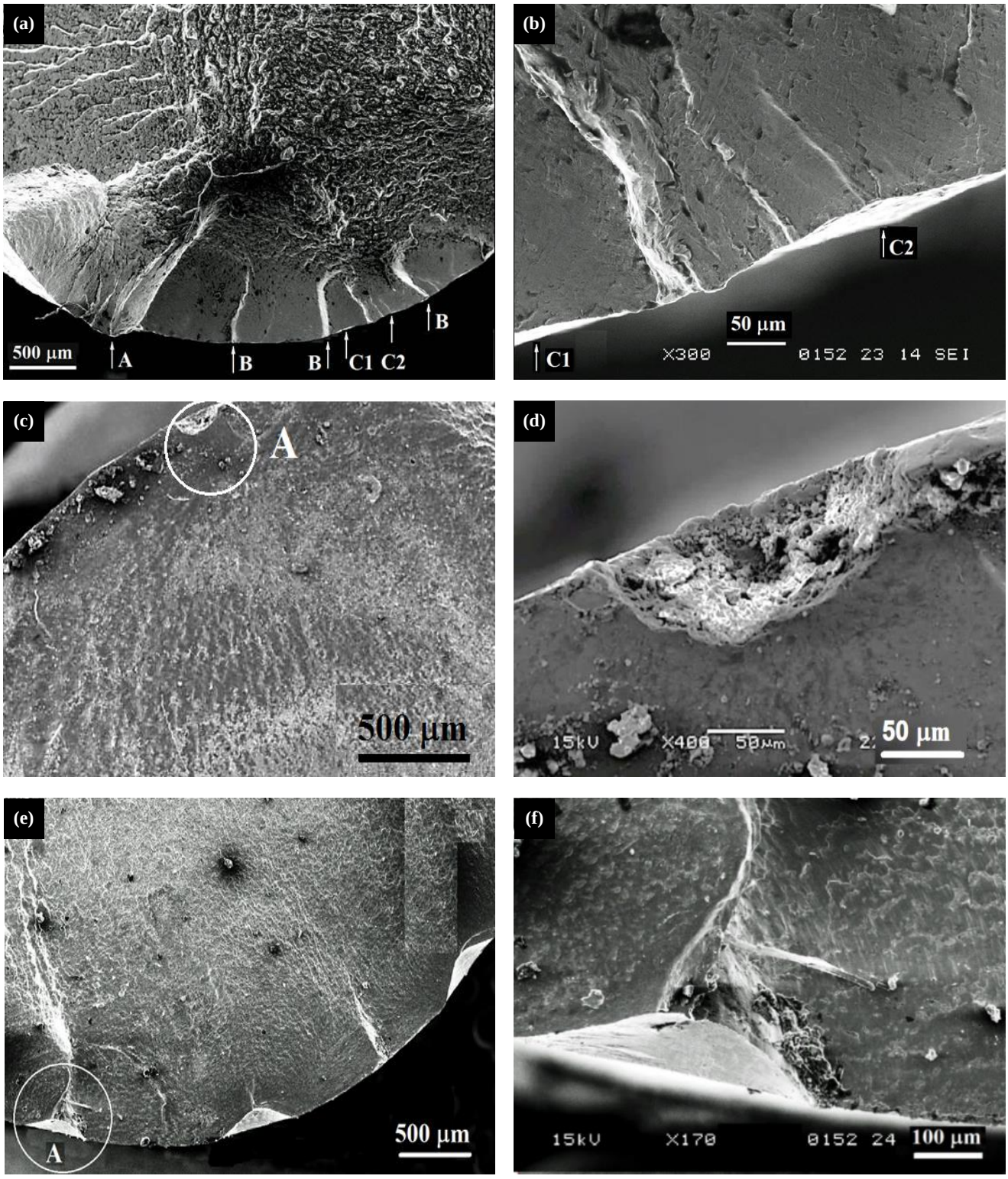

Figure 8. SEM micrographs of the fracture surface of samples without (a, b) and with artificial defects, which caused the failure of samples 26 (a, b), 36 (c, d), and 18 (e, f). (a, b) - two craters C1 and C2 as a result of shot peening (group 3, 821.5 MPa, $N_f = 0.66 \times 10^5$ cycles); (c, d) - the EDM-made defect (group 3b, 729 MPa, $N_f = 2.2 \times 10^5$ cycles); (e, f) - three prints of hardness tests, (group 2b, 624.8 MPa, $N_f = 2 \times 10^7$ cycles); (b, d, f) - magnification of areas 'A'.

The indentations obtained during the Rockwell hardness tests had blunt tips, which undoubtedly did not correspond to the radius of the sharp tip of the 120° conical diamond indenter. Sharp tips in the indentations after the hardness test were blunt due to plastic deformation of the steel, both during the stress relaxation process before the fatigue test and during the latter. This #18 sample showed no fracture during the HCF test, but after that it was tensile ruptured to demonstrate where a crack could occur. The indentations produce a strong strengthening effect, resulting in a much longer time to failure of the fatigue specimen. For example, as shown in Figure 8(e) and (f), three indentations in the center of specimen 18 were the sites of initiation of cracks capable of rapidly moving deeper into the specimen; however, it had a much longer time to failure ($N_f = 2 \times 10^7$ cycles) compared to the average N_f value of 8×10^5 cycles for samples 7 and 8 without artificial defects at the same applied stress 624.8 MPa (Table 2). Here, experiment 15 is not taken into consideration, in which corrosion pits of small depth and relatively large diameter were obtained. In this case, apparently, the preliminary anodic dissolution of iron in a salt solution was rather closer to electrochemical polishing than to the creation of an artificial defect. Therefore, this sample showed a slightly longer fatigue life ($N_f = 10.08 \times 10^5$) compared to an average value of $N_f = 8.04 \times 10^5$ for samples 7 and 8 without artificial defects (Table 2).

It is of interest to consider the topography of the fatigue fracture of samples with defects, obtained as a result of the preliminary corrosion in solutions of perchloric acid and 3.5% NaCl (Figure 9 and Figure 10). The size and shape of the pits obtained by anodic dissolution of steel in an electrochemical cell mainly depends on voltage and current, as well as on the type of electrolyte. Crack initiation in samples during fatigue experiments seems to be easier in the pits produced by corrosion in perchloric acid than in the pits formed in sodium chloride solution, due to the smoother shape of the latter (Figure 2). Moreover, despite the fact that pit A in Figure 9(a) seems smooth and rounded, it was a source of fatigue failure of sample L9. The cross-section of sample 22 passing through one of the pits near the fracture surface shows that a stress concentrator was located at the bottom of the pit, which led to the formation of a secondary crack (Figure 9(b)). Similar secondary cracks can also be seen in pit A in Figure 9(a).

As was shown in Figure 5 for samples of group 2a, the parameter $\sqrt{area}$ plays a decisive role in fatigue life. For example, two samples of this group (Nos.15 and 17) with pits A obtained as a result of pre-corrosion in 3.5% NaCl (Table 2, Figure 10(a) and (b) showed that the fatigue life decreases from 10.08×10^5 cycles to 1.19×10^5 cycles or by an order of magnitude with an increase in $\sqrt{\text{area}}$ from 0.13 mm to 0.18 mm. In each sample, the first cracks initiated from two adjacent pits A located at a distance of less than 0.5 mm (Figure 10(a) and (b).

Let us also consider the features of fatigue failure of samples of group 1a (Nos. L5, L7 and L9) consisted of pits, formed as a result of anodic dissolution of steel in perchloric acid (Figure 10(c) and (f). The ridges in Figure 10(d) and 10 g clearly indicate where cracks occurred. At an applied stress of 520.7 MPa, samples No. L5 and L7 with a pit diameter of 0.17 mm and 0.16 mm, respectively, had a fatigue life of 0.87×10^5 cycles and 0.60×10^5 cycles versus 1.3×10^5 cycles for sample No. L9 with pit A, which had a diameter of 0.08 mm (these tests were performed previously without depth measurement). In the left corner of Figure 10(e), there is the image showing an oval pit A, in the lower part of which you can see a deep hole as the source of the main crack, causing fatigue failure.

Summarizing the above, it can be noted that the roughness is a critical factor for the fatigue properties of the steel. The surface quality improving leads to a marked increase in the fatigue life and fatigue limit. The fatigue life of specimens with artificial defects of various sizes, taken into account by in $\sqrt{\text{area}}$ parameter, is significantly reduced. Defects obtained due to electrochemical corrosion had a much greater detrimental effect on fatigue life compared to other defects. In general, shot peening improves fatigue performance of the steel. First of all, as reported in [8-10,13,23], this is due to the creation of a compressive field of residual stresses in the surface layer of the metal, on which a tensile - compressive load can be applied during bending fatigue tests, in particular, at stress ratio R = -1. The residual compressive stress on the surface of 4320 steel after shot peening, performed according to parameters similar to this study, is about -1000 MPa and reduces to zero at a depth of 0.15-0.20 mm [23].

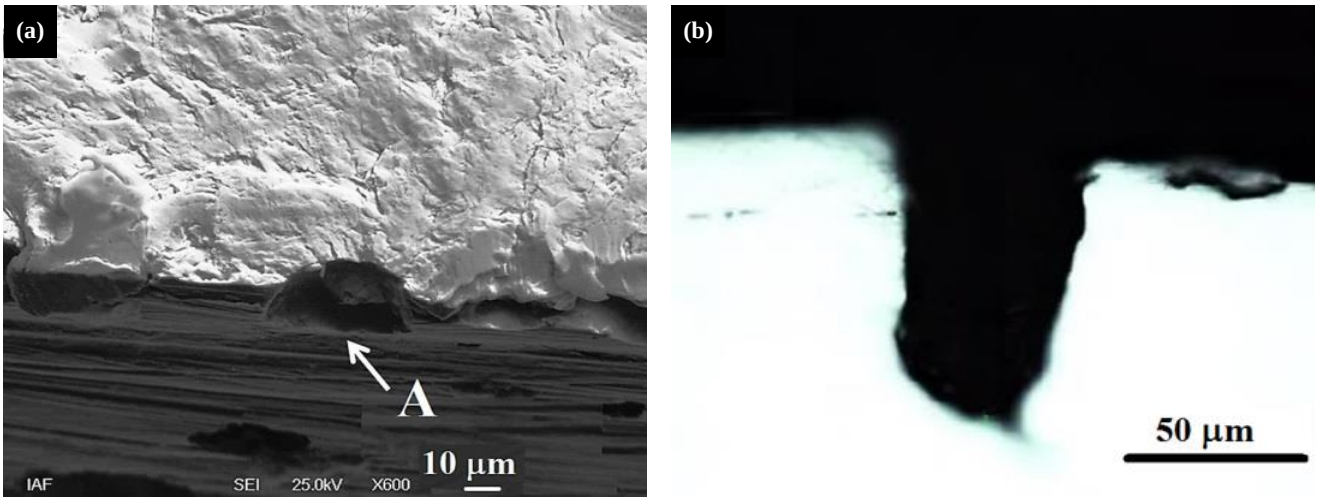

Figure 9. Pits previously obtained in a perchloric acid solution after fatigue failure. (a) - SEM image of the fracture surface of sample L9 with the pit A (group 1, 520.7 MPa, $N_f = 1.3 \times 10^5$); (b) - optical micrograph of a cross-section of sample No. 22 near the fracture surface (group 3c, 729 MPa, $N_f = 3 \times 10^5$).

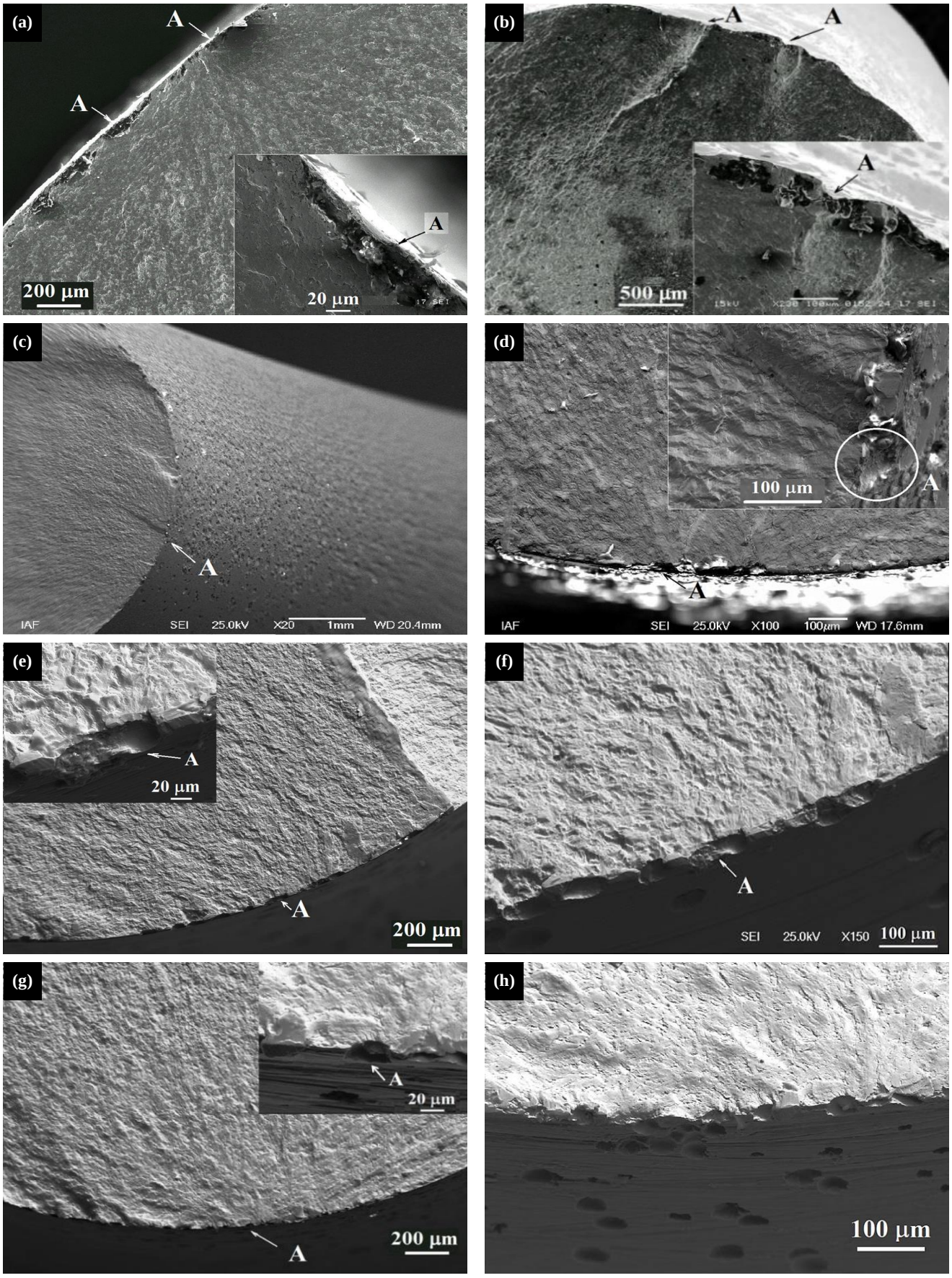

Figure 10. SEM images of the fatigue fracture surfaces of samples showing pits A that were previously obtained using corrosion in solutions of (a, b) NaCl and (c-h) perchloric acid, and were sources of fatigue failure. (a, b): samples of group 2a, 624.8 MPa; (a) - No.15 ($N_f = 1.1\times10^6$) and (b) - No.17 ($N_f = 0.12 \times 10^6$); (c-h): samples of group 1a, 520.7 MPa, including (c, d) - No.L5 ($N_f = 0.87 \times 10^5$); (e, f) - No.L7 ($N_f = 0.6 \times 10^5$) and (g, h) - No.L9 ($N_f = 1.3\times10^5$).

4. Conclusions

1. The roughness R_a of the samples is a critical factor for the fatigue performance of tempered low alloy steel 4340. A sixfold increase in fatigue life was found with a reduction in roughness from 1.6 μm to 0.4 μm. Additionally, shot peening of specimens resulted in an increase in N_f by more than threefold.

2. The fatigue limit (strength) increases by 16% with a decrease in Ra from 1.6 μm to 0.4 μm, and by about 14% with shot peening of the steel with the same initial roughness of 0.4 μm.

3. Several types of artificial surface defects were performed on the steel specimens with a subsequent rotation fatigue test. The fatigue life of specimens with artificial defects of various sizes, taken into account by the $\sqrt{\text{area}}$ parameter, is significantly reduced.

4. Shot peening has a positive effect on fatigue resistance even in the presence of corrosion pits. However, even SP does not completely eliminate the negative effects of corrosion pits on fatigue resistance. Defects obtained by electrochemical corrosion had a much greater detrimental effect on fatigue life compared to defects obtained using the EDM technique or by indentation.

Acknowledgements

Authors would like to thank A. Jarashneli, E. Kolmakov, H. Didi, and A. Krein (Ben-Gurion University of the Negev, Israel) for their kind assistance in specimen preparation, fatigue tests, and microscopy.

References

[1] Y.-L. Lee, I. Pan, R. Hathaway, and M. Barkey, *Fatigue testing and analysis (Theory and Practice)*, Amsterdam, Boston-Tokyo: Elsevier Inc., 2005.

[2] S. R. Lampman, "*Fatigue and Fracture",* in ASM Handbook, ASM International, Metals Park, OH, pp. 596-597, 1996.

[3] Y. Murakami, and M. Endo, "Quantitative evaluation of fatigue strength of metals containing various small defects or cracks," *Engineering Fracture Mechanics*, vol. 17, pp.1-15, 1983.

[4] Y. Murakami, and M. Endo, "Effects of defects, inclusions and inhomogeneities on fatigue strength," *Fatigue*, vol. 16, pp. 163-182, 1994.

[5] J. T. Cammett, and P. S. Prevey, "Fatigue strength restoration in corrosion pitted 4340 alloy steel via low plasticity burnishing," *Lambda Research, Cincinnati, OH, report*, 10 p., 2006.

[6] J. Sakamoto, Y. Takahashi, Y. Aono, and H. Noguchi, "Method for assessing applicability of an artificial flaw as a small initial crack for fatigue limit evaluation and its application to a drill hole and an FIB processed sharp notch in annealed 0.45% carbon steel," *Journal of Test Evaluation*, vol. 41, no. 2, pp.1-7, 2013.

[7] B. M. Schönbauer, K. Yanase, and M. Endo, "The influence of various types of small defects on the fatigue limit of precipitation-hardened 17-4PH stainless steel". *International Journal of Fatigue*, vol. 100, pp. 540-548, 2017.

[8] J. Sakamoto, Y.-S. Lee, and S.-K. Cheong, "Effect of surface flaw on fatigue strength of shot-peened medium - carbon steel," *Engineering Fracture Mechanics*, vol. 133, pp. 99-111, 2015.

[9] K. Takahashi, T. Amano, K. Ando, and F. Takahashi, "Improvement of fatigue limit by shot peening for high-strength steel containing a crack-like surface defect," *International Journal of Structural Integrity*, vol. 2, no. 3, pp. 281-292, 2011.

[10] I. Fernández-Pariente, S. Bagherifard, M. Guagliano, and R. Ghelichi, "Fatigue behavior of nitrided and shot peened steel with artificial small surface defects," *Engineering Fracture Mechanics*, vol. 103, pp. 2-9, 2013.

[11] J. R. Donahue, and J. T. Burns," Effect of chloride concentration on the corrosion–fatigue crack behavior of an age-hardenable martensitic stainless steel," *International Journal of Fatigue*, vol. 91, Part 1, pp.79-99, 2016.

[12] S.I. Rokhlin, and J.-Y. Kim, "In situ ultrasonic monitoring of surface fatigue crack initiation and growth from surface cavity," *International Journal of Fatigue*, vol. 25, pp. 41-49, 2003.

[13] S. Baiker, *Shot Peening: A Dynamic Application and Its Future*, Ed., Publisher, MFN -Metal Finishing News, 182 p., 2006.

[14] Procedures for Using Standard Shot Peening Test Strip: SAE J443 JAN84 SAE recommended practice. Amer. Nation. Standards Inst., Society of Automotive Engineers, 4 p. 1985.

[15] D. Wu, C. Yao, and D. Zhang, "Surface characterization and fatigue evaluation in GH4169 superalloy: Comparing results after finish turning; shot peening and surface polishing treatments," International Journal of Fatigue, vol. 113, pp. 222-235, 2018.

[16] ASTM E1558, "Standard Guide for Electrolytic Polishing of Metallographic Specimens", Publ. ASTM, Dec. 1999.

[17] H. Itoga, K. Tokaji, M. Nakajima, and H.-N. Ko, "Effect of surface roughness on step-wise S–N characteristics in high strength steel," *International Journal of Fatigue*, vol. 25 pp. 379-385, 2003.

[18] M. Suraratchai, J. Limido, C. Mabru, and R. Chieragatti, "Modelling the influence of machined surface roughness on the fatigue life of aluminium alloy," International Journal of Fatigue, vol. 30, no. 12, pp. 2119-2126, 2008.

[19] H. Masuo, Y. Tanaka, S. Morokoshi, H. Yagura, T. Uchida, Y. Yamamoto, and Y. Murakami, "Influence of defects, surface roughness and HIP on the fatigue strength of Ti-6Al-4V manufactured by additive manufacturing," *International Journal of Fatigue*, vol. 117, pp. 163-179, 2018.

[20] M. F. Garwood, H. H. Zurburg, and M. A. Erickson. "Correlation of laboratory tests and service performance," in: Interpretation of tests and correlation with service, *American Society for Metals*, Ch. 1, pp. 1-77, 1951.

[21] Y. Murakami, "Material defects as the basis of fatigue design," *International Journal of Fatigue*, vol. 41, pp. 2-10, 2012.

[22] V. Kerlins, Modes of Fracture, ASM Handbook, vol 12: Fractography, ASM International, pp. 12-71, 1987. DOI: 10.31399/asm.hb.v12.a0001831.

[23] M. A. S. Torres, and H. J. Cvoorwald, "An evaluation of shot peening, residual stress and stress relaxation on the fatigue life of AISI 4340 steel," International Journal of Fatigue, vol. 24, no. 8, pp. 877-886, 2002.